Published in final edited form as:
*Biomaterials*. 2012 November ; 33(33): 8372–8382. doi:10.1016/j.biomaterials.2012.08.021.

# Selective functionalization of nanofiber scaffolds to regulate salivary gland epithelial cell proliferation and polarity

**Shraddha I. Cantara**[a], **David A. Soscia**[b], **Sharon Sequeira**[a], **Riffard Jean-Gilles**[a], **James Castracane**[b], and **Melinda Larsen**[a,*]

[a]Dept. of Biological Sciences, University at Albany, State University of New York, 1400 Washington Street, Life Sciences Bldg, Albany, NY 12222

[b]College of Nanoscale Science and Engineering, University at Albany, State University of New York, 257 Fuller Road, Albany, NY 12203

## Abstract

Epithelial cell types typically lose apicobasal polarity when cultured on 2D substrates, but apicobasal polarity is required for directional secretion by secretory cells, such as salivary gland acinar cells. We cultured salivary gland epithelial cells on poly(lactic-co-glycolic acid) (PLGA) nanofiber scaffolds that mimic the basement membrane, a specialized extracellular matrix, and examined cell proliferation and apicobasal polarization. Although cells proliferated on nanofibers, chitosan-coated nanofiber scaffolds stimulated proliferation of salivary gland epithelial cells. Although apicobasal cell polarity was promoted by the nanofiber scaffolds relative to flat surfaces, as determined by the apical localization of ZO-1, it was antagonized by the presence of chitosan. Neither salivary gland acinar nor ductal cells fully polarized on the nanofiber scaffolds, as determined by the homogenous membrane distribution of the mature tight junction marker, occludin. However, nanofiber scaffolds chemically functionalized with the basement membrane protein, laminin-111, promoted more mature tight junctions, as determined by apical localization of occludin but did not affect cell proliferation. To emulate the multifunctional capabilities of the basement membrane, bifunctional PLGA nanofibers were generated. Both acinar and ductal cell lines responded to signals provided by bifunctional scaffolds coupled to chitosan and laminin-111, demonstrating the applicability of such scaffolds for epithelial cell types.

### Keywords

laminin-111; chitosan; nanofibers; salivary gland; epithelial cells; polarity

## 1. Introduction

The salivary glands are required for producing saliva to lubricate the oral cavity, maintain the oral tissues, initiate the process of digestion and initiate an immune response against invaders that enter through the oral cavity [1]. The submandibular salivary gland contains



*Corresponding author mlarsen@albany.edu, Fax: (518) 442-4767.

Supplementary Materials
Supplementary material associated with this article can accessed online at doi….

two major epithelial cell types that produce saliva: acinar cells and ductal cells. Acinar cells produce saliva while ductal cells modify the saliva composition and transport the saliva into the oral cavity [2]. Both cell types are required for production of normal saliva. Both acinar and ductal epithelial cells are apicobasally polarized, and maintenance of this structure is critical for directional secretory function [3]. In the adult salivary gland, most epithelial cells have a basement membrane located on the basal side and a lumen on the apical side. Apicobasal polarity of such cells is maintained primarily by tight junctions (TJ) with some contribution by adherens junctions (AJs). TJs are complexes of proteins including the transmembrane proteins, claudins and occludin, and the cytoplasmic scaffolding protein, ZO-1, that are associated with the apical region of the lateral membrane of polarized epithelial cells [4,5,6].

*In vivo*, epithelial cells rest upon a fibrous network of secreted proteins, carbohydrates, and other molecules, known as the basement membrane [7] that is largely assembled by these cells. The components of the basement membrane provide signals to cells to induce and maintain apicobasal polarity [7,8]. Laminin proteins, primary components of the basement membrane, have been shown to be required for establishment and maintenance of apicobasal polarity in a variety of epithelial cell types, including renal and dental epithelia [9].

Several approaches to engineering salivary gland tissue have been proposed, and one approach is to culture cells on a scaffold, which provides signals to cells from the basal side. Salivary gland cell proliferative responses to films composed of polyvinyl alcohol (PVA), poly (ethylene-co-vinyl alcohol) (EVAL) or polyvinylidene fluoride (PVDF) have been tested [10]; however, this study did not examine cell polarity, which is important for cell function. Although culture of salivary gland cells on Matrigel, an exogenous basement membrane derived from a murine tumor [11], demonstrated that Matrigel stimulates apicobasal polarity in salivary gland cells [8], this material is impractical for *in vivo* implantation in humans. Scaffold that can direct epithelial cell behavior will be necessary for engineering a functional salivary gland.

Many polymeric and natural materials have been engineered to create scaffolds having nanoscale features that replicate structures in natural cell environments. While nanofiber scaffolds have been used extensively as scaffolds for mesenchymal cells to mimic the extracellular matrix, few studies have investigated their utility for epithelial cells. We previously generated poly-lactic-co-glycolic acid (PLGA) scaffolds to mimic the fibrillar characteristics of the basement membrane and showed that SIMS cells, a salivary gland ductal epithelial cell line, can attach and proliferate on these PLGA nanofiber scaffolds [12]. Additionally, the morphology of SIMS cells and PARC10 cells, an acinar salivary gland cell line, cultured on the nanofibers more closely resembled that of adult salivary gland cells *in vivo*. These cells self-organized into clusters and exhibited less cell spreading, as expected of epithelial cells in vivo. Additionally, the epithelial cells produced fewer organized focal adhesions, which are typically produced by mesenchymal cells and also by cells cultured on flat artificial flat surfaces [13]. Thus, the PLGA nanofiber scaffolds appeared to support epithelial cell morphology; however the effect on apicobasal polarity was not determined.

In this study, we covalently attached molecules to the nanofiber scaffolds to “functionalize” the scaffolds to better replicate the properties of native basement membrane. We attached two molecules to the scaffolds, both individually and in combination, to modulate cell proliferation and cell polarity independently: chitosan, a deactylated form of the crustacean exoskeleton molecule, and the basement membrane protein, laminin-111. We examined the responses of salivary gland acinar and ductal cells to the functionalized scaffolds by examining both cell proliferation and apicobasal polarity.

## 2. Materials and Methods

### 2.1 Cell Culture

Two immortalized salivary gland cell lines were used: SIMS cells, an immortalized mouse ductal submandibular epithelial cell line [14] and SMGC10 cells, an immortalized rat parotid acinar epithelial cell line [15]. SIMS cells were cultured in Dulbecco's High Glucose Modified Eagle Medium (DMEM) (Invitrogen Cat No. 11995) supplemented with 10% Heat-Inactivated Fetal Bovine Serum (HI FBS) (Invitrogen Cat No. 10082) and Penicillin-Streptomycin (1×) (Invitrogen Cat. No. 15140). SMGC10 cells were cultured as previously published [15] with minor modifications in Dulbecco's Modified Eagle Medium (DMEM)/F-12 with Phenol Red, 15mM HEPES, and L-Glutamine (Invitrogen Cat No. 11330) supplemented with 5μg/ml insulin (Sigma Cat No. 16634), 0.1μM retinoic acid (Sigma Cat No. 2625), 2nM L-3,5,3′-triiodothyronine ($T_3$) (Sigma Cat No. T-5516), 1μM hydrocortisone (Sigma Cat No. H-0135), 4μg/ml transferrin (Invitrogen Cat No. 11105-021), 50ηg/ml epithelial growth factor (EGF), (Peprotech Cat No.CYT-217), 2mM glutamine (Invitrogen Cat No. 11330), trace element mix (MilliPore Cat No. 1676649), 50μg/ml gentamicin (Invitrogen Cat No. 15710-064), and 2.5% HI FBS. Both cell types were maintained in 10cm polystyrene tissue culture plates (Corning Cat. No. 430167) at 37°C with 5% $CO_2$ in a humidified incubator and passaged at 80–90% confluence.

### 2.2 Making of PLGA fiber scaffolds and film

PLGA fiber scaffold were generated by electrospinning using a design of experiment (DOE) approach, as previously described [12, 13]. Briefly, PLGA polymer containing a lactic to glycolic acid ratio of 85:15 and a molecular weight of 95,000 Da (Birmingham Polymers) was dissolved in hexafluoroisopropanol (HFIP) with 1% NaCl (w/v); an 8% (w/w) solution was used for nanofibers while an 18% solution was used for microfibers. The polymer solutions were ejected out of a syringe using an automated syringe pump at a flow rate of 3 μL/min for nanofibers and 10 μL/min for microfibers. Constant voltage was provided by attaching a wire from the power supply to the needle. Voltage for nanofibers was 10kV while voltage for microfibers was 12kV. The needle was suspended vertically over a grounded aluminum collector plate at a distance of 15cm. Pre-cleaned 12mm diameter glass coverslips (Deckglaser Cat No. 1001/12) were coated with Vectabond (Vectabond Laboratories) and 50μl of solvent-casted 3% PLGA polymer solution was pipetted upon aluminum foil over the collector plate and dried for 1 hour so that fibers could attach to coverslips. PLGA film was made by applying 80μL of 5% PLGA polymer solution dissolved in chloroform per 12mm Vectabond-coated glass coverslip and spincoating them. The coverslips were spun at 1500rpm for 1 min and then placed upon a 200°C hotplate until the solvent evaporated. All scaffolds were sterilized using UV irradiation, washed and incubated in sterile 1×PBS supplemented with 1× Penicillin-Streptomycin, and incubated in sterile cell culture media for 48 hours prior to use in experiments, as we reported previously [13].

### 2.3 Nanofiber Modifications

Electrospun PLGA fiber scaffolds were modified with either FITC-chitosan or laminin-111 prior to cell seeding. PLGA fiber scaffolds were hydrolyzed by incubation in a 50mM NaOH solution for 30min at room temperature. Then scaffolds were activated by incubating in 4mM 1-ethyl-3-(3-dimethylaminopropyl) carbodiimide (EDAC) (Sigma Aldrich Cat No. 39391), 100mM Nhydroxysuccinimide (NHS) (Sigma Aldrich Cat No. 130672), 10mM 2-(N-morpholino) ethanesulfonic acid (MES) solution (Sigma Aldrich Cat No. M1317) for 1hr at room temperature, as reported previously [16]. These chemical treatments did not significantly affect the fiber macrostructure, as determined by SEM (data not shown). Next, scaffolds were incubated in either a 1% FITC-chitosan solution in 0.1M acetic acid or a

10μg/mL laminin-111 (Sigma Aldrich Cat No. L2020) solution in cold 1× PBS at 4°C overnight. To confirm attachment of FITC-chitosan, confocal images were acquired (Leica TCS SP5)). To confirm attachment of laminin-111, fiber scaffolds were immunostained with anti-laminin antibody and observed with confocal microscopy (Leica TCS SP5). All scaffolds were washed and incubated in sterile 1×PBS supplemented with 1× penicillin-streptomycin, and incubated in sterile cell culture media prior to use in experiments.

### 2.4 Proliferation Assay

Cells were seeded in 24-well polystyrene, flat-bottom tissue culture plates (Becton-Dickinson Cat No. 353047) at a density of $1.5\times10^4$ cells/ml and cultured for up to 72 hours. At 12, 24, 48, and 72 hours, cells were washed with 1×PBS, detached using 0.25% Trypsin-EDTA, neutralized with cell culture media, and collected in microcentrifuge tubes. Cells were centrifuged for 5 minutes at 500 rpm; the supernatant was discarded, and pellets were resuspended in 0.4% trypan blue dye in media (Invitrogen Cat No. 15250) for 10 minutes before counting. Live and dead cells were counted using a hemocytometer. Graphs were produced using Microsoft Excel. Statistical analysis was performed using GraphPad Prism software. A p value $< 0.05$, as determined by one-way ANOVA analysis with Bonferroni post-test, was considered to be statistically significant.

### 2.5 Immunocytochemistry and Confocal Microscopy

Cells were seeded on 12mm glass coverslips or coverslips coated with nanofibers in 24-well plates, cultured for 48 hours, and immunostained as described previously [13]. Primary antibodies used included mouse anti-ZO-1 (Invitrogen Cat No. 339100), mouse anti-occludin (Invitrogen Cat No. 33-1500), rabbit anti-aquaporin 5 (Alamone labs Cat No. (AQP5-005), rat anti-CD49f (Integrin α6) (BD Pharmingen Cat No. 555734), and rabbit anti-laminin-111 (Novus Biologicals 300-144). Secondary antibody solutions included 4′, 6-diamidino-2-phenylindole, dihydrochloride (DAPI) (Molecular Probes Cat. No. D1306) and rhodamine phalloidin (Invitrogen Cat No. R415) with Cy2-donkey anti-mouse (Jackson IR Cat No.715-226-150), Cy5-donkey anti-rat (Jackson IR Cat No.712-176-150), and Cy3-donkey anti-rabbit (Jackson IR Cat No.711-166-152), as required. Primary and secondary antibodies were previously validated for specificity and minimal background staining with immunocytochemistry. Coverslips were mounted using FLUORO-GEL with Tris buffer mounting media (Electron Microscopy Science Cat No. 17985-10). Cells were imaged using the Leica TCS SP5 confocal microscope at the College of Nanoscale Science and Technology (CNSE). Images were collected at 20× and 63× (oil). Z-stack images were collected using a 0.5μm step size over an average distance of approximately 5.5μm and analyzed using Leica Software LASAF (Leica Microsystems Inc.). The same laser settings were used to compare protein expression levels in cells seeded on different scaffolds in the same experiment. Apical and basal images were selected by detection of specified apical and basal marker proteins, β-actin and integrin α6, respectively.

### 2.6 Immunoblotting

Cells were seeded at a density of $5.0\times10^4$ cells/ml on different scaffolds in 24-well plates and cultured for 48 hours. Whole cell lysates (5–10 μg protein/lane) were collected using RIPA buffer, and total protein amounts quantified using a MicroBCA™ Protein Assay Kit (Thermo Scientific Cat No. 23235), as previously described [13]. 10-well or 15-well precast 4–15% Mini PROTEAN®TGX™ gels (Biorad Cat No. 465-1083, 465-1086) were used for immunoblotting. Primary antibodies used included mouse anti-ZO-1, mouse anti-β-actin (Sigma Aldrich Cat No. A3853), and mouse anti-GAPDH (Fitzgerald Labs Cat No. 10R-G109a). Secondary antibodies used include Horseradish peroxidase (HRP) anti-mouse IgG (GE/Amersham Cat No. NXA931) and HRP anti-rabbit IgG (GE/Amersham Cat No. NA934). Western blots were developed and analyzed, as previously described [13]. All data

was calculated and graphed in Microsoft Excel. Statistical analysis was performed using GraphPad Prism software. In one-way ANOVA analysis with Bonferroni Post-tests, a p value $< 0.05$ was considered to be statistically significant.

## 3. Results

### 3.1 Unmodified PLGA nanofiber scaffolds

Epithelial cells must form a confluent sheet of polarized cells in the context of a secretory organ to achieve directional secretion [17]. We previously generated polymeric, nanofiber scaffolds composed of poly(lactic-co-glycolic acid) (PLGA) as a structural mimic of the basement membrane, a specialized extracellular matrix, as a scaffold for salivary gland epithelial cell lines [12,13]. We seeded a ductal (SIMS) salivary gland cell line on PLGA nanofiber scaffolds and examined the effects on cell proliferation. Cells cultured on PLGA nanofibers proliferated more than cells on flat substrates (glass and film) (Figure 1A), as we observed previously [12]; however, to generate a full monolayer, it was necessary to further stimulate cell proliferation.

### 3.2 Nanofiber chemical modifications-chitosan

Chitosan, a deactylated form of the crustacean exoskeleton molecule, chitin that has been used in many biomedical applications, was previously shown to stimulate the developmental process of branching morphogenesis in embryonic submandibular salivary gland organ explants [18]. Chitosan is structurally similar to glucosaminoglycans (GAGs), which are natural components of the basement membrane and extracellular matrix [19] that are known to influence cell proliferation [20,21]. In human skin fibroblasts and keratinocytes [22] and salivary acinar cells [10] chitosan has been shown to increase cell proliferation. We observed that chitosan-supplemented growth media stimulated SIMS cell proliferation (data not shown). Therefore, chitosan was chemically coupled to the nanofiber scaffolds to examine its affects on salivary gland cell proliferation in this context. FITC-chitosan was covalently attached to electrospun PLGA fiber scaffolds following a series of hydrolysis and activation steps involving EDAC/NHS chemistry, as described in materials and methods. Fluorescence microscopy verified that chitosan had been successfully coupled to PLGA nanofibers since a relatively homogenous fluorescence of the fibers was detected (Figure 2).

### 3.3 Chitosan's effects on SIMS salivary gland ductal cell proliferation

Proliferation assays were used to determine if chitosan, as a scaffold modification, promoted proliferation of salivary gland epithelial cells. SIMS cells were cultured for 12, 24, 48, and 72 hours on chitosan-modified and unmodified scaffolds as well as on flat substrate (glass and PLGA film) controls. Live and dead cells were counted; total viable cells and percent viability were plotted (Figure 1A & 1B). Total cell number increased over time on all substrates tested, as expected for proliferating cells; however, chitosan significantly stimulated cell proliferation moreso than the nanofibers themselves (Figure 1A). Percent viability for cells cultured on all substrates remained relatively constant over the 72 hour time period (Figure 1B), indicating no toxicity stimulated by chitosan. Chitosan was also incorporated into the nanofibers as a pre-electrospinning modification (Supplementary Figure 1A), which involved addition of FITC-chitosan to the PLGA solution and a modification of previously established parameters for electrospinning nanofiber scaffolds, as described in Jean-Gilles et. al. 2010 [12]. SIMS cell proliferative and polarity responses were tested on pre-and post-electrospun, chitosan-modified nanofibers. SIMS cells proliferated equally well on both types of chitosan-modified fibers while viability was unaffected by any treatment (Supplementary Figure 1B & C). Since chitosan modification of the nanofibers was equally as effective either as a pre- or post-electrospinning modification

of the nanofibers, the post-electrospinning modification method was used in subsequent experiments.

### 3.4 Effects of chitosan on SIMS cell polarity

Once epithelial cells have proliferated on a flat scaffold to form a monolayer, the cells should subsequently undergo apicobasal polarization. Since adult mouse submandibular salivary glands demonstrate apical localization of ZO-1 (Figure 3A), a tight junction and adherens junction scaffolding protein [23], we examined the expression of ZO-1 in cells cultured on nanofibers. Immunoblotting was used to quantify ZO-1 expression in SIMS cells cultured on post-electrospinning chitosan-modified and unmodified nanofibers and compared to cells cultured on glass or PLGA film after 48 hours (Figure 4). Although ZO-1 expression levels slightly decreased for chitosan-modified nanofibers relative to non-modified nanofibers, statistical analysis from three independent experiments indicated no significant differences ($p>0.05$) between protein levels in cells cultured on any substrate type (Figure 4).

ZO-1 localizes to the cytoplasmic face of the apical region of the lateral membrane in AJ and TJ in polarized epithelial cells. To examine the localization of ZO-1 in cells cultured on modified or unmodified scaffolds, immunocytochemistry and confocal imaging was used; the localization was compared to that of cells in mouse submandibular gland (SMG) tissue. In embryonic day 13 (E13) mouse SMGs, ZO-1 was dispersed throughout the plasma membrane in epithelial cells in immature buds, as reported previously [24], but was apically restricted in epithelial cells in adult glands (Figure 3A). Integrin α6 was used as a basal marker (data not shown) and an enhanced concentration of filamentous β-actin was used to detect the apical cell border (Figure 5D). Z stacks of images captured using confocal imaging confirmed that ZO-1 protein was randomly distributed adjacent to plasma membranes of SIMS cells cultured on chitosan-modified nanofibers (Figure 5A), although SIMS cells cultured only on unmodified nanofibers showed apical restriction of ZO-1 (Figure 5A) similar to the adult gland. Regardless of whether chitosan was added to the nanofibers pre- or post-electrospinning, ZO-1 was uniformly distributed adjacent to the plasma membrane (Supplementary Figure 2A).

Mature TJ localized to the apical region of the lateral membrane contain both the integral membrane proteins, claudins and occludins. Occludin (Guillemot 2008) is apically localized in mature tight junctions in both adult SMG aquaporin 5-postitive acinar and aquaporin 5-negative ductal cells but is only sparsely localized in the buds of immature E13 glands (Figure 3B). Occludin was randomly distributed both on apical and basal membranes of cells cultured on all substrate types (Figure 5B and Supplementary Figure 2B). This data suggests that chitosan disrupts apical ZO-1 localization, which is promoted by the unmodified nanofibers, and that nanofibers cannot promote the formation of mature TJ, as detected by occludin localization.

### 3.5 Nanofiber chemical modifications-laminin-111

To further promote the apicobasal polarity of salivary epithelial cells, additional scaffold modifications were investigated. Since basement membrane proteins in the laminin family have been shown to be required for establishment and maintenance of polarity in a variety of epithelial cell types, including renal and dental epithelia [9], we hypothesized that laminin-111-coated nanofiber scaffolds might further promote apicobasal polarity. Specifically, laminin-111-coated nanofiber scaffolds promoted apical restriction of the TJ protein occludin in SIMS cells (Figure 6B), that is apically localized in acini and ducts in adult SMG tissue (Figure 3B). Laminin-111 was covalently linked to PLGA nanofiber scaffolds through hydrolysis and activation steps involving EDAC/NHS chemistry [16], as

described in materials and methods. To verify coupling of laminin-111 to the PLGA nanofiber scaffolds, the modified scaffolds were immunostained and visualized using fluorescence microscopy. Fluorescence microscopy demonstrated that laminin-111 was successfully coupled to PLGA nanofibers as a relatively homogenous fluorescence of the fibers was detected after the coupling reaction (Figure 2).

### 3.6 Effects of laminin-111 on cell polarity of ductal and acinar cells

To determine if laminin-111, as a scaffold modification, promoted epithelial cell apicobasal polarity, immunocytochemistry was used to localize ZO-1 and occludin in SIMS cells cultured for 48 hours on unmodified and laminin-111-modified nanofiber scaffolds. ZO-1 was homogenously distributed around the cell periphery of SIMS cells, cultured on all substrates (Figure 6A), similar to its distribution in cells cultured on the flat substrate control (Figure 6A). As previously noted, SIMS cells grown on unmodified nanofibers showed apical restriction of ZO-1 (Figure 6A), and this apical localization was maintained on laminin-111-modified nanofibers (Figure 6A). To determine if the laminin-111 modification could promote the maturation of tight junctions, cells were immunostained for occludin. Interestingly, occludin was apically restricted in cells cultured on laminin-111 but not in cells seeded on any other scaffolds (Figure 6B). Since the SIMs cells are a ductal-derived cell line, we examined the effect of laminin-111 on the apicobasal polarization of an acinar cell line, SMGC10. SMGC10 cells responded similarly to the SIMS cells in that ZO-1 became apically restricted in cells grown on the unmodified scaffolds, but laminin-111 was required to achieve apical occludin (Figure 7). This data suggests that laminin-111-modification of the nanofibers promotes the maturation of tight junctions in both acinar and ductal cell lines, thereby enhancing apicobasal polarity in both of these cell types.

### 3.7 Effects of laminin-111 on cell proliferation

Since laminin-111 promotes apicobasal polarization, we hypothesized that laminin-111 might halt cell proliferation. Therefore, we tested the effects of laminin-111 on SIMS and SMGC10 proliferation and cell viability. As in previous experiments, cells were cultured for 12, 24, 48, and 72 hours on laminin-111-modified and unmodified scaffolds and flat substrate controls. Live and dead cells were counted, and this data was used to calculate total number of cells and percent viability (Figure 8). As observed previously, total cell numbers increased on all substrates over time for SIMS cells and similarly for SMGC10 cells, (Figures 8A & 8C), and the nanofiber scaffolds significantly promoted cell proliferation moreso than the flat substrates after 48hrs. Laminin-111, as a scaffold modification, did not affect either SIMS or SMGC10 cell proliferation or cell viability over the 72 hour time period (Figure 8B & 8D). This data indicates that laminin-111 does not affect SIMS or SMGC10 cell proliferation or viability.

### 3.8 Effects of doubly-labeled nanofibers on SIMS cell polarity

Since chitosan and laminin-111 both elicit differing cellular responses from salivary gland cells, we investigated whether the cells would respond to the simultaneous presentation of both modifications. We chemically modified nanofiber scaffolds with both chitosan and laminin-111 (Figure 2) and grew SIMS cells on them. Immunocytochemistry was used to detect ZO-1 localization in SIMS cells on chitosan and laminin-111-modified nanofibers (Figure 9). As observed previously, ZO-1 was uniformly distributed proximal to the lateral cell membrane in the cells grown on flat substrates and on chitosan-modified nanofibers (Figure 9A). In contrast, cells grown on unmodified nanofibers and on laminin-111-modified nanofibers showed apical restriction of ZO-1, and cells grown on the chitosan/laminin-111 nanofibers showed an intermediate phenotype (Figure 9A). This data indicates that the cells respond to both chitosan and laminin-111 in the context of a doubly modified nanofiber scaffold. The distribution of occludin also indicated that the cells could respond to

both chitosan and laminin-111 on the fibers. Occludin was fully apically restricted in SIMS cells only when the cells were cultured on laminin-111-modified nanofibers (Figure 9B). Cells on doubly modified fibers showed an intermediate phenotype; although some apical accumulation of occludin was detected, occludin was not excluded from the basal region of the lateral membrane (Figure 9B). These data indicate that salivary epithelial cells can respond to multiple signals in the context of a complex chemically modified nanofiber scaffold.

## 4. Discussion

Current treatments for xerostomia, or “dry mouth” resulting from salivary hypofunction are inadequate as long-term therapies due to the inconvenience of constant application, unpleasant side effects, and inefficiency in stimulating salivation from severely damaged salivary glands [1]. An artificial salivary gland could provide an improved quality of life to patients suffering from salivary hypofunction. An essential characteristic of secretory epithelial cells is apicobasal polarity. Cell-cell junctions, such as AJ and TJ, are required to mediate the maturation of an epithelial sheet and are required for establishment of apicobasal polarity [23]. Both AJ and TJ are dynamic, multimolecular, multifunctional complexes. AJ are formed first as epithelial cells establish cell-cell contacts in developing tissues [23]. We here report that PLGA nanofiber scaffolds can promote the apical localization of ZO-1, primarily a TJ scaffolding protein [26] that regulates TJ assembly through recruitment of other TJ proteins, such as claudins, and occludin [25], that is also associated with AJ [23]. The unmodified nanofiber scaffolds perhaps make the cells competent to form TJs even though TJ remain immature in cells cultured on them. Our results are consistent with a recent study in which poly lactic acid (PLA) electrospun nanofibers stimulated polarization of primary neuronal cells [27].

Chitosan was hypothesized to stimulate cell proliferation due to its structural similarity to glycosaminoglycans, which can recruit growth factors to the cell surface [21]. Cell proliferation increased for cells cultured on chitosan-modified nanofibers with no decrease in cell viability, consistent with several other studies that have shown a positive effect of chitosan on cell proliferation [22,28] although the mechanism has not been elucidated. In the epithelial cells used in our study, it is not clear whether chitosan might stimulate the recruitment of growth factors or stimulate production of autocrine-acting growth factors. Interestingly, apicobasal polarity, initiated by nanofibers, was disrupted by chitosan, as ZO-1 localization was not apically restricted in cells cultured in the presence of chitosan. This implies that chitosan may directly oppose polarity signals or it may activate cell proliferation to indirectly inhibit apicobasal polarity. Considering the later possibility, maturation of cells though establishment of apicobasal polarity and subsequent differentiation is typically paralleled by a reduction in cell proliferation [29].

Our results show that apicobasal polarity, initiated by nanofibers, is enhanced by laminin-111, as the mature TJ protein, occludin, was apically restricted in cells grown on laminin-111-modified nanofibers. These results are consistent with other studies that indicate that laminin induces epithelial cell polarity. In one study, laminin-511 was found to be required for dental epithelial cell polarity [30]. A recent study from our laboratory showed that Matrigel can induce apicobasal polarity in SIMS salivary gland epithelial cells. When SIMS cells were seeded on Matrigel, which is an exogenous matrix that contains large quantities of basement membrane proteins including laminin-111, cells became significantly more polarized, as detected by apical localization of ZO-1 [8]. Since Matrigel is approximately 70% laminin [11], it is likely that laminin plays a major role in promoting polarity, which is corroborated by the current study. Interestingly, SIMS cell proliferation

was not affected by laminin-111 in this study, even though cell differentiation stimulated by basement membrane is frequently paralleled by a decrease in cell proliferative rates.

Nanofiber scaffolds were designed to physically imitate the basement membrane, but PLGA alone lacks specific chemical signals found in the basement membrane. Functionalization of the PLGA nanofiber scaffold with multiple signaling molecules would theoretically produce a scaffold that more closely resembles *in vivo* basement membrane. When we cultured cells on nanofibers modified with both laminin-111 and chitosan we found that these cells show an intermediate polarity phenotype, implying that cells can sense and respond to both molecules. It would therefore be desirable to design future scaffolds in which such chemical signals can be delivered sequentially. The proliferative signal should be delivered to cells first to stimulate cell proliferation and stimulate full cell occupation of the scaffold, followed by subsequent unmasking of a cell polarization signal. In future work, coupling of additional bioactive molecules might make it possible to stimulate salivary stem/progenitor cells to undergo differentiation into specific functional epithelial cell subtypes.

## 5. Conclusions

In this study, we found that unmodified PLGA nanofiber scaffolds provide signals to salivary gland epithelial cells to both proliferate and to initiate apicobasal polarity in culture. These signals were enhanced by covalent coupling of chitosan and/or laminin-111 to the nanofibers. Chitosan enhanced cell proliferation but disrupted apicobasal localization of ZO-1 stimulated by the nanofibers. Laminin-111 promoted apicobasal polarity through stimulation of apical localization of TJ proteins, including ZO-1 and occludin, indicative of mature TJ formation in both salivary gland acinar and ductal cells. Cells were capable of responding to both laminin-111 and chitosan modifications to the nanofibers. This work demonstrates the capability of modified nanofiber scaffolds to provide chemical signals to epithelial cells that support cell proliferation and apicobasal polarity, which indicates their feasibility for use in future engineering of an artificial salivary gland or other organ containing epithelial tissues.

## Supplementary Material

Refer to Web version on PubMed Central for supplementary material.

## Acknowledgments

The authors would like to thank Drs. Mary Reyland and David Quissell for gifts of the SMGC10 cells and Dr. Daniel Malamud for the SIMS cells. Dr. Nathaniel Cady for assistance with the Leica SP5 Confocal Microscope. This work was supported by NIH grants R21DE019197, R21DE01919702S1, and R01DE022467 to M.L. and J.C., R01DE019244 and RC1DE020402 to M.L., NSF Contract # DV10922830 to J.C., and C06 RR015464 to the University at Albany, SUNY.

## References

1. Ship JA. Diagnosing, managing, and preventing salivary gland disorders. Oral Dis. 2002; 8(2):77–89. [PubMed: 11991308]
2. Tucker AS. Salivary gland development. Semin Cell Dev Biol. 2007; 18(2):237–44. [PubMed: 17336109]
3. Handler JS. Overview of oral epithelia. Annu Rev Physiol. 1989; 51:729–40. [PubMed: 2653202]
4. Gumbiner B. Structure, biochemistry, and assembly of epithelial tight junctions. Am J Physiol. 1987; 253(6):749–58.
5. Furuse M, Hirase T, Itoh M, Nagafuchi A, Yonemura S, Tsukita S. Occludin: a novel integral membrane protein localizing at tight junctions. J Cell Biol. 1993; 123(6):1777–88. [PubMed: 8276896]

6. Baker OJ. Tight junctions in salivary epithelium. J Biomed Biotechnol. 2010; 2010:278–91.
7. Patel VN, Rebustini IT, Hoffman MP. Salivary gland branching morphogenesis. Differentiation. 2006; 74(7):349–64. [PubMed: 16916374]
8. Daley WP, Gervais EM, Centanni SW, Gulfo KM, Nelson DA, Larsen M. ROCK1-directed basement membrane positioning coordinates epithelial tissue polarity. Development. 2012; 139(2): 411–22. [PubMed: 22186730]
9. Klein G, Langegger M, Timpl R, Ekblom P. Role of laminin A chain in the development of epithelial cell polarity. Cell. 1988; 55:331–41. [PubMed: 3048705]
10. Chen MH, Hsu YH, Lin CP, Chen YJ, Young TH. Interactions of acinar cells on biomaterials with various surface properties. J Biomed Mater Res Part A. 2005; 74(2):254–62.
11. Kleinman HK, Martin GR. Matrigel: basement membrane matrix with biological activity. Semin Cancer Biol. 2005; 15(5):378–86. [PubMed: 15975825]
12. Jean-Gilles R, Soscia D, Sequeira S, Melfi M, Gadre A, Castracane J, et al. Novel modeling approach to generate a polymeric nanofiber scaffold for salivary gland cells. J Nanotechnol Eng Med. 2010; 1:1–10.
13. Sequeira SJ, Soscia DA, Oztan B, Mosier AP, Jean-Gilles R, Gadre A, et al. The regulation of focal adhesion complex formation and salivary gland epithelial cell organization by nanofibrous PLGA scaffolds. Biomaterials. 2012; 33(11):3175–86. [PubMed: 22285464]
14. Laoide BM, Courty Y, Gastinne I, Thibaut C, Kellermann O, Rougeon F. Immortalised mouse submandibular epithelial cell lines retain polarized structural and functional properties. J Cell Sci. 1996; 109:2789–800. [PubMed: 9013327]
15. Quissell DO, Barzen KA, Gruenert DC, Redman RS, Camden JM, Turner JT. Development and characterization of SV40 immortalized rat submandibular acinar cell lines. In vitro Cell Dev Biol. 1997; 33(3):164–73.
16. Koh HS, Yong T, Chan CK, Ramakrishna S. Enhancement of neurite outgrowth using nano-structured scaffolds coupled with laminin. Biomaterials. 2008; 29:3574–82. [PubMed: 18533251]
17. Aframian DJ, Palmon A. Current status of the development of an artificial salivary gland. Tissue Eng Part B. 2008; 14(2):187–98.
18. Yang TL, Young TH. The enhancement of submandibular gland branch formation on chitosan membranes. Biomaterials. 2008; 29:2501–8. [PubMed: 18316118]
19. Cummings, RD.; Varki, A.; Esko, JD. Essentials of gylcobiology. 2. Vol. Chapter 16. Cold Spring Harbor Laboratory Press; 2009.
20. Ruozi B, Parma B, Croce MA, Tosi G, Bondioli L, Vismara S, et al. Collagen-based modified membranes for tissue engineering: influence of type and molecular weight of GAGs on cell proliferation. Int J Pharm. 2009; 378:108–15. [PubMed: 19501149]
21. Trowbridge JM, Rudisill JA, Ron D, Gallo RL. Dermatan sulfate binds and potentiates activity of keratinocyte growth factor (FGF-7). J Biol Chem. 2002; 277(45):42815–20. [PubMed: 12215437]
22. Howling GI, Dettmar PW, Goddard PA, Hampson FC, Dornish M, Wood EJ. The effect of chitin and chitosan on the proliferation of human skin fibroblasts and keratinocytes in vitro. Biomaterials. 2001; 22:2959–66. [PubMed: 11575470]
23. Hartsock A, Nelson WJ. Adherens and tight junctions: structure, function and connections to the actin cytoskeleton. Biochim Biophys Acta. 2008; 1778(3):660–9. [PubMed: 17854762]
24. Hieda Y, Iwai K, Morita T, Nakanishi Y. Mouse embryonic submandibular gland epithelium loses its tissue intergrity during early branching morphogenesis. Dev Dyn. 1996; 207:395–403. [PubMed: 8950514]
25. Fanning AS, Anderson JM. Zonula occludens-1 and -2 are cytosolic scaffolds that regulate the assembly of cellular junctions. Ann N Y Acad Sci. 2009; 1165:113–20. [PubMed: 19538295]
26. Guillemot L, Paschoud S, Pulimeno P, Foglia A, Citi S. The cytoplasmic plaque of tight junctions: a scaffolding and signalling center. Biochim Biophys Acta. 2008; 1778(3):601–13. [PubMed: 18339298]
27. Gertz CC, Leach MK, Birrell LK, Martin DC, Feldman EL, Corey JM. Accelerated neuritogenesis and maturation of primary spinal motor neurons in response to nanofibers. Dev Neurobiol. 2010; 70(8):589–603. [PubMed: 20213755]

28. Ueno H, Nakamura F, Murakami M, Okumura M, Kadosawa T, Fujinaga T. Evaluation effects of chitosan for the extracellular matrix production by fibroblasts and the growth factors production by macrophages. Biomaterials. 2001; 22(15):2125–30. [PubMed: 11432592]
29. Lima WR, Parreira KS, Devuyst O, Caplanusi A, N'kuli F, Marien B, et al. ZONAB promotes proliferation and represses differentiation of proximal tubule epithelial cells. J Am Soc Nephrol. 2010; 21(3):478–88. [PubMed: 20133480]
30. Fukumoto S, Miner JH, Ida H, Fukumoto E, Yuasa K, Miyazaki H, et al. Laminin alpha5 is required for dental epithelium growth and polarity and the development of tooth bud and shape. J Biol Chem. 2006; 281(8):5008–16. [PubMed: 16365040]

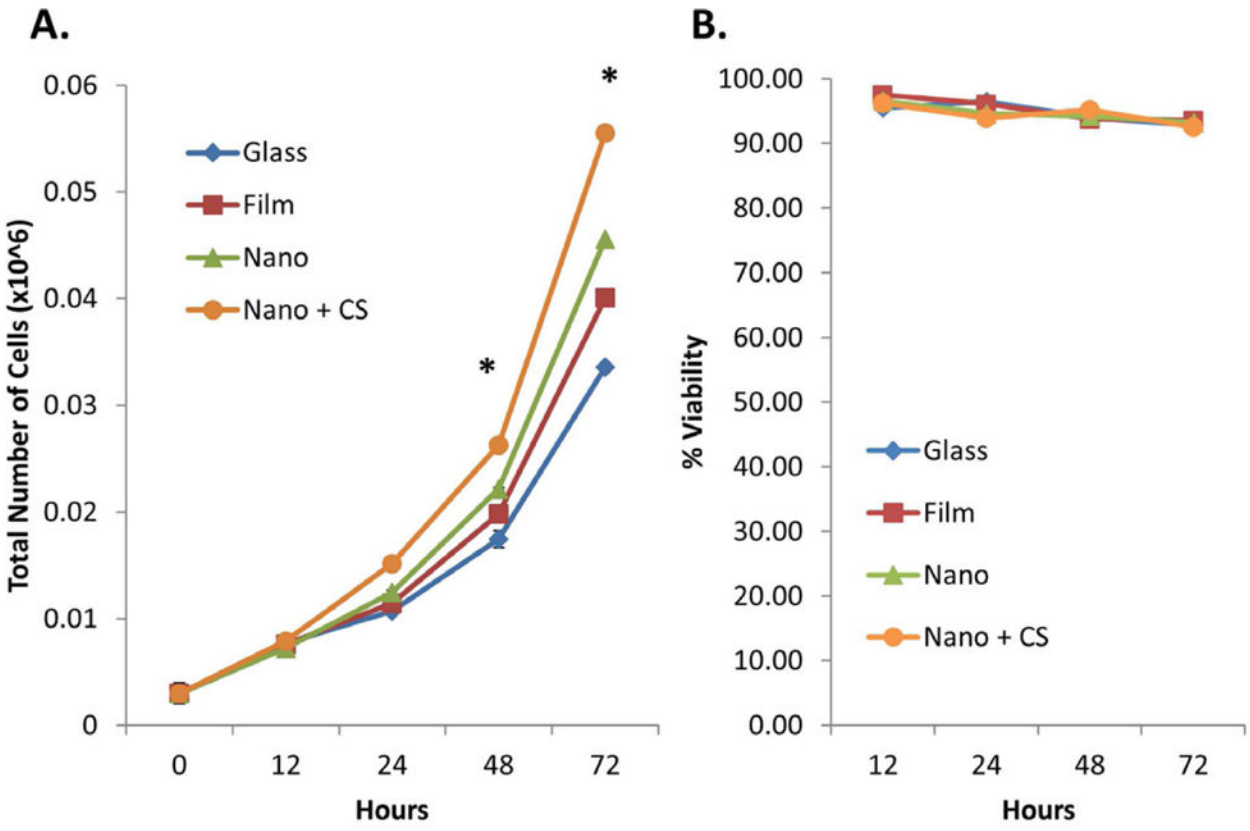


**Figure 1.**

Chitosan modification of nanofibers increases SIMS cell proliferation but does not affect cell viability. **(A)** Increased cell proliferation was observed for cells cultured on chitosan-modified scaffolds as compared with cells cultured on unmodified nanofibers and flat substrate controls for 12-72 hrs. Mean ± SEM of 2 experiments. One-way ANOVA with Bonferroni post tests indicate a significant difference (* $p<0.05$) between cells grown on chitosan-modified nanofibers and unmodified nanofibers at 48 and 72 hours. **(B)** % cell viability is not adversely affected for cells cultured on any substrates at any time point. Mean ± SEM of 2 experiments. One-way ANOVA with Bonferroni post-tests results indicate no significant difference ($p>0.05$) between cells on any substrate type at any time point.

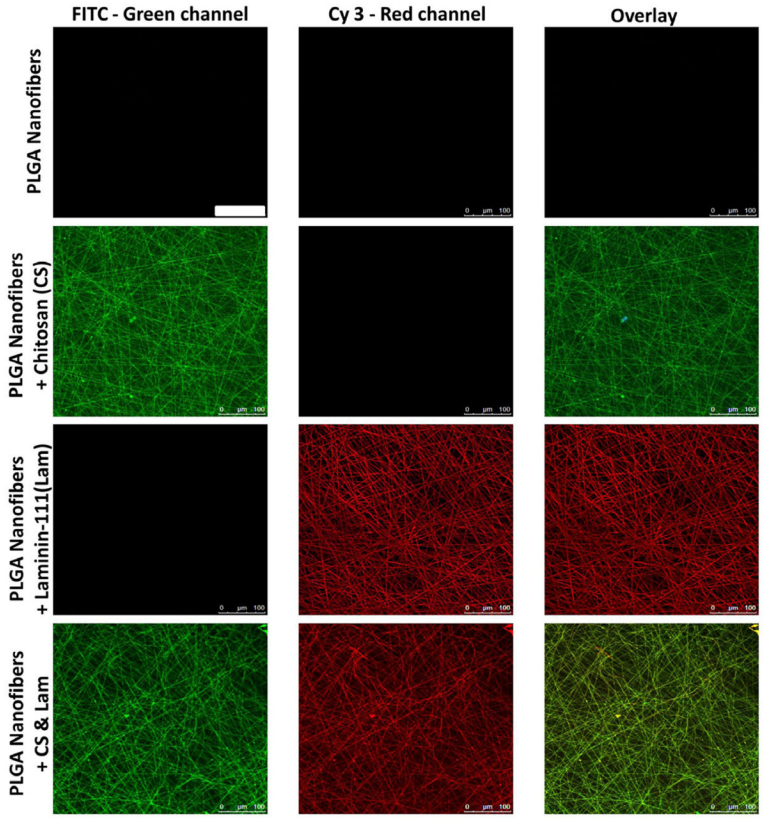


**Figure 2.**
PLGA fiber scaffolds modified with chitosan and/or laminin-111 post-electrospinning. Fluorescence microscopy of unmodified, FITC-chitosan modified, laminin-111-modified, and chitosan- and laminin-111-modified PLGA fiber scaffolds prepared with the post-electrospinning method. Confocal images demonstrate FITC-chitosan labeling (green) and laminin-111 labeling detected by immunostaining (red). Scale, 100 μm.

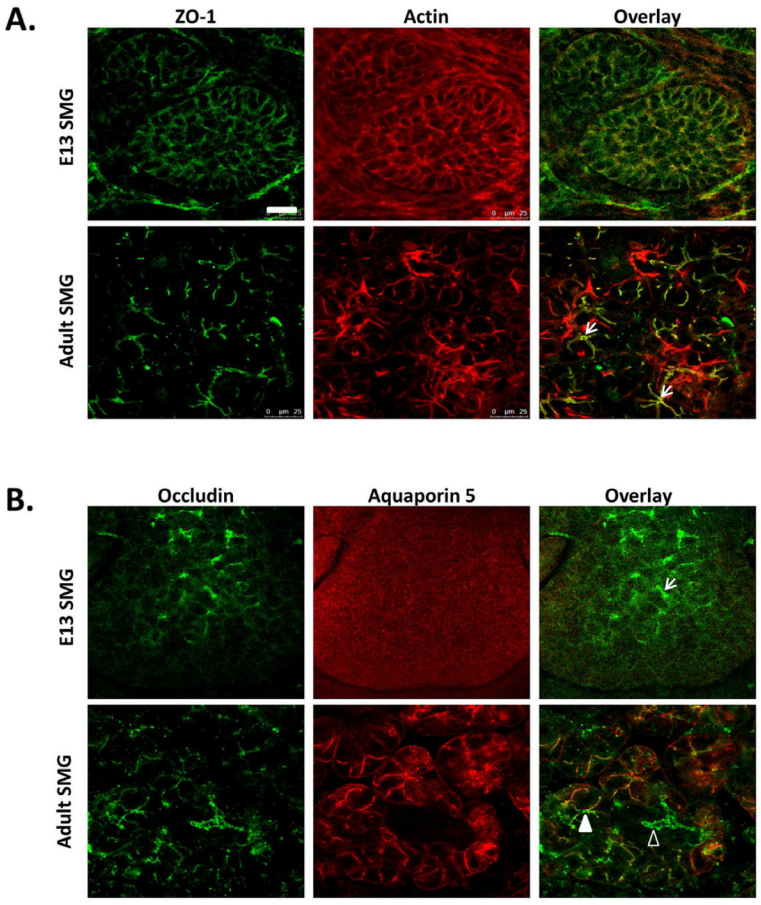


**Figure 3.**

Tight junction protein localization in embryonic day 13 (E13) and adult submandibular salivary glands (SMG). Immunostaining and confocal images show **(A)** ZO-1 and β-actin in E13 and adult SMG. ZO-1 is distributed around all plasma membranes in epithelial buds with few areas of localization in E13 SMG but is focally concentrated at apical membranes in adult tissue adjacent to apical concentrations of β-actin (arrows). **(B)** Occludin and aquaporin 5 (Aqp5) localization in E13 and adult SMGs. In E13 SMGs, occludin is detected only in a few focal areas in undifferentiated buds showing no localized Aqp5 (arrows). In adult SMG, occludin is apically concentrated in both ducts (Aqp5 negative, open arrowheads) and in acini (Aqp5 positive, solid arrowheads).

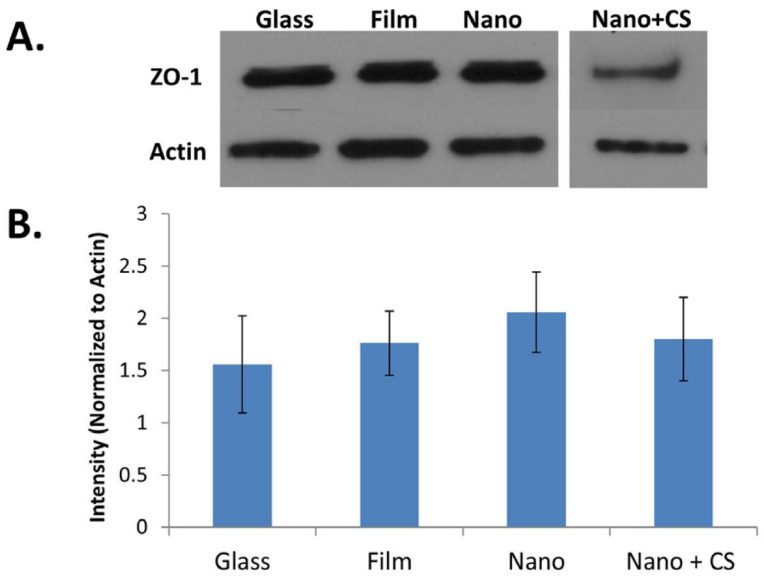


**Figure 4.**

Chitosan-modified nanofibers do not affect ZO-1 protein expression in SIMS salivary gland ductal cells. **(A)** Western blots in which ZO-1 (220kDa) and β-actin (45kDa) (loading control) bands were detected to quantify ZO-1 protein expression in SIMS cells after 48 hours of culture. **(B)** Graph of quantified ZO-1 expression, normalized to β-actin. Mean ± SEM of 3 experiments. One-way ANOVA with Bonferroni post test results indicate no significant difference in levels of ZO-1 in cells grown on nanofibers, modified nanofibers, or flat controls, $p>0.05$.

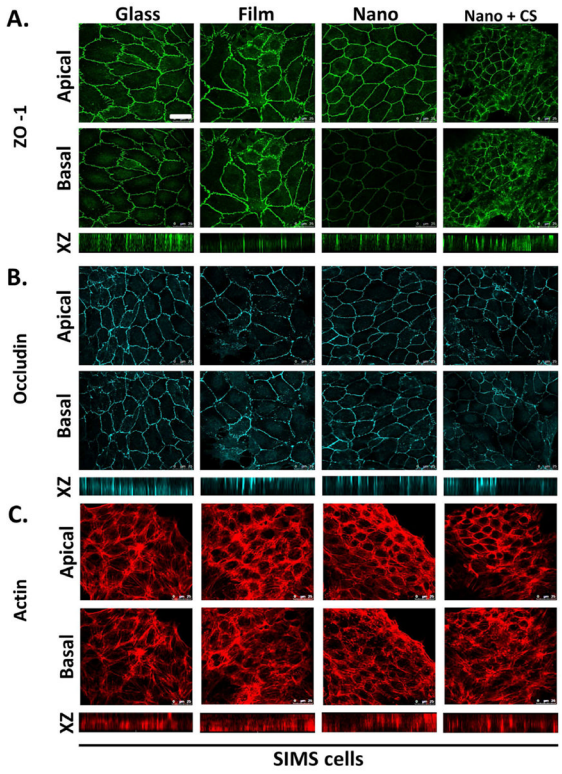


**Figure 5.**

PLGA nanofibers promote apical restriction of ZO-1, which is disrupted by chitosan. Immunostaining detected **(A)** ZO-1 and **(B)** occludin localization. **(C)** The actin cytoskeleton was detected using rhodamine-phalloidin. Representative single confocal (63×) images were selected from Z-stacks to represent apical and basal sections of SIMS cells on the basis of β-actin and integrin α6 localization (data not shown). XZ projections provide a vertical view of protein localization throughout the height of the cell. SIMS cells seeded on nanofibers fibers showed restriction of ZO-1 but not occludin to the apical side of the cell, which is indicative of AJ but not mature TJ formation. Chitosan-modified nanofiber scaffolds disrupted the apical restriction of ZO-1. Scale, 25 μm.

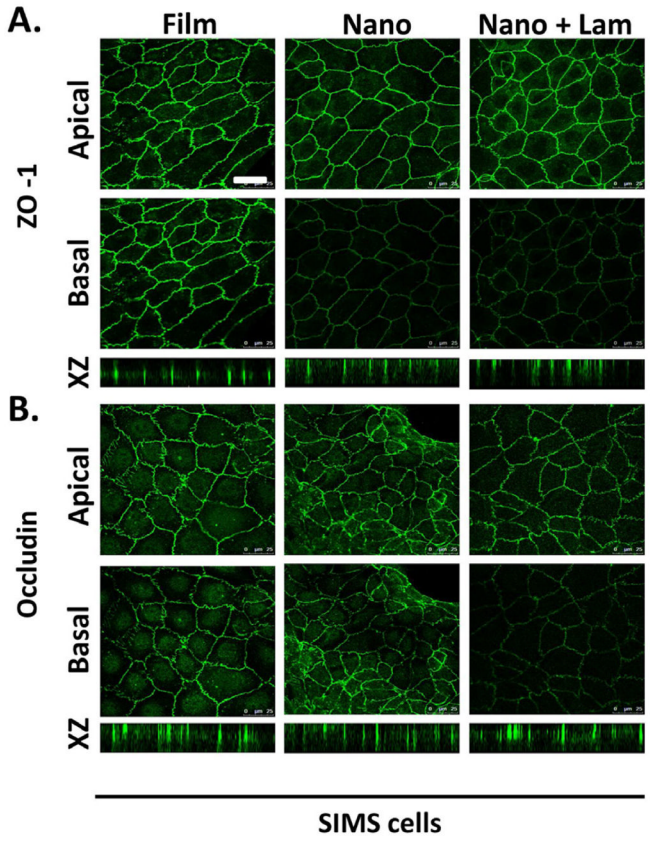


**Figure 6.**

Laminin-111 modification of nanofibers enhances polarity of SIMS cells. Cells were immunostained for **(A)** ZO-1 and **(B)** occludin as indicators of apicobasal polarity. Single apical and basal confocal images and XZ projections indicate that both ZO-1 and occludin are apically localized in the presence of laminin-111, which is indicative of TJ maturation. Scale, 25 μm.

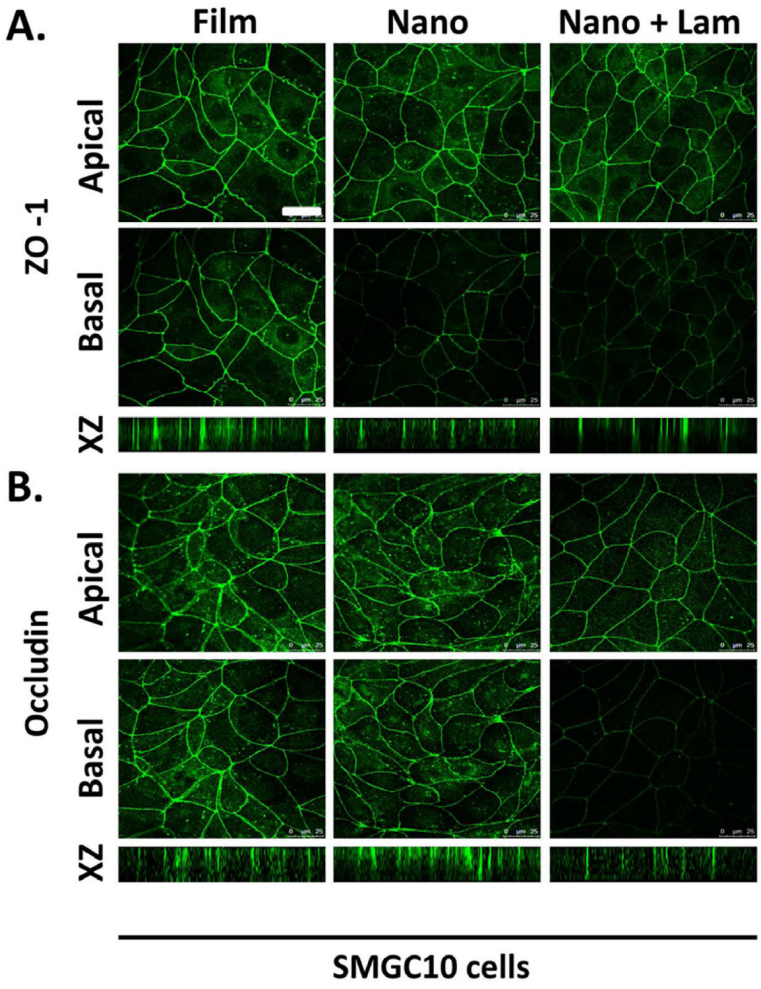


**Figure 7.**

Laminin-111 modification of nanofibers enhances polarity of SMGC10 salivary gland acinar cells. Cells were immunostained for **(A)** ZO-1 and **(B)** occludin, as indicators of apicobasal polarity. Single apical and basal confocal images and XZ projections indicate that both ZO-1 and occludin are apically localized in the presence of laminin-111, which is indicative of TJ formation. Scale, 25 μm.

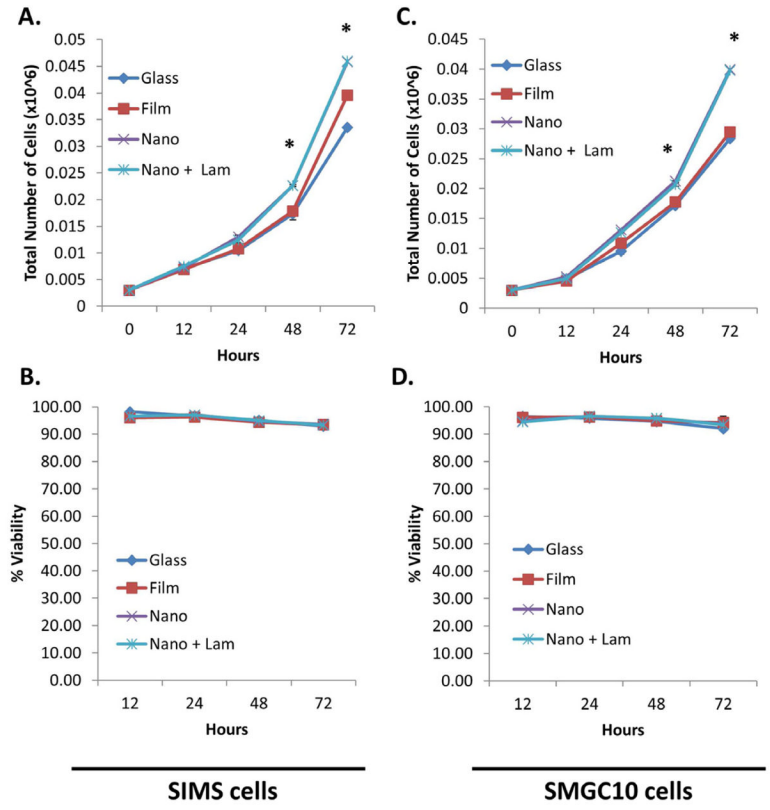


**Figure 8.**

Laminin-111-modified nanofibers increase ductal (SIMS) and acinar (SMGC1O) cell proliferation without affecting cell viability. Total cell number graphs showing increased **(A)** SIMS cell and **(B)** SMGC10 cell proliferation for cells cultured on laminin-111-modified scaffolds as compared to unmodified nanofibers and flat substrate controls from 12–72 hrs. Mean ± SEM of 2 experiments. One-way ANOVA with Bonferroni post-tests indicates a significant difference (* $p<0.05$) between nanofibers (unmodified and laminin-111-modified) and flat substrates (glass and PLGA film) at 48 and 72 hours. Cells cultured on laminin-111-modified vs. unmodified nanofibers did not show a difference in proliferation rate. Graphs for % viability of **(C)** SIMS and **(D)** SMGC10 cells show that viability is not affected by the laminin-111 coating. Mean ± SEM of 2 experiments. One-way ANOVA with Bonferroni post test results indicate no significant difference in viability ($p>0.05$) for all substrate types at all time points.

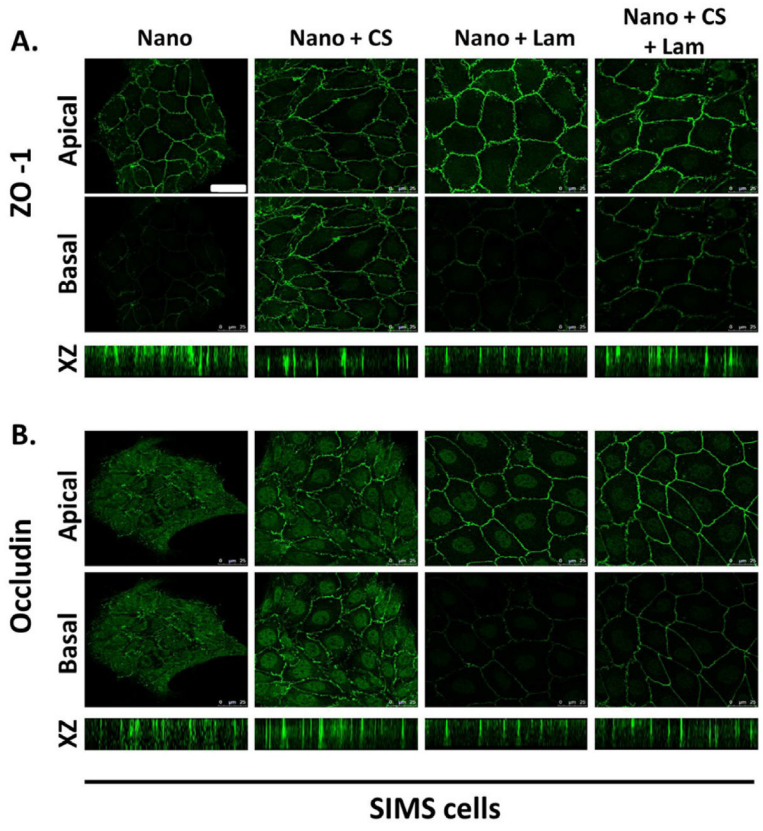


**Figure 9.**

Bifunctional nanofibers induce an intermediate polarity phenotype in SIMS ductal cells. SIMS cells were cultured for 48 hours on nanofibers, chitosan-coated fibers, laminin-111-coated fibers, or chitosan and laminin-111- coated fibers. Cells were immunostained for **(A)** ZO-1 and **(B)** occludin as apical polarity markers. Single confocal images were chosen from Z-stacks to represent apical and basal regions of SIMS cells. Bifunctional nanofiber scaffolds promote the apical restriction of ZO-1 and occludin but not to the same extent as laminin-111-modified fibers alone, since the cells also respond to the non-polarizing chitosan signal. Scale, 25 μm.